American Journal of
Biomedical Science & Research

www.biomedgrid.com
ISSN: 2642-1747

Research Article

Influence of Gelatin Bloom Grade and Crosslinker Dose on Particle Size in One- and Two-Step Desolvation, With Preliminary Evidence of Uptake by A549 Cells

Emmanuella Rony[1], Adrian McCollum[2], Jesse Edwards[3*] and Jillian Pope[1,3*]

[1]*Department of Chemistry, Florida A&M University, Tallahassee, FL 32307, USA*

[2]*Department of Biology, Florida A&M University, Tallahassee, FL 32307, USA*

[3]*Department of Chemistry, Morgan State University, Baltimore, MD 21251, USA*

***Corresponding author:** Jesse Edwards & Jillian Pope, Department of Chemistry, Morgan State University, Baltimore, MD 21251, USA & Florida A&M University, Tallahassee, FL 32307, USA.

To Cite This article: *Emmanuella Rony, Adrian McCollum, Jesse Edwards* and Jillian Pope*, Influence of Gelatin Bloom Grade and Crosslinker Dose on Particle Size in One- and Two-Step Desolvation, With Preliminary Evidence of Uptake by A549 Cells. Am J Biomed Sci & Res. 2026 31(6) AJBSR.MS.ID.004103,* **DOI:** 10.34297/AJBSR.2026.31.004103

Received: August 04, 2026 **Published:** August 14, 2026

Abstract

Gelatin is an attractive nanoparticle matrix for drug delivery and imaging because it is collagen-derived, biodegradable, inexpensive, and of low antigenicity. Additionally, particle size is tunable through the desolvation process itself rather than through post-synthetic fractionation. Here, Type B bovine gelatin of two Bloom grades (75 and 225) was converted to nanoparticles by one-step and two-step desolvation with acetone at pH 2.5 and 60°C, crosslinked with glutaraldehyde, purified by dialysis against water, and characterized by dynamic light scattering with morphological confirmation by atomic force microscopy. Fluorescent preparations were made by labeling gelatin with Fluorescein-5-Isothiocyanate (FITC) in borate buffer before desolvation, and their association with A549 human lung adenocarcinoma cells was examined by confocal laser scanning microscopy after 24h. Size effects are reported as internally controlled ordinal comparisons rather than as absolute diameters. Two synthesis variables dominated the outcome. Bloom grade determined the direction of the size difference: in both the one-step and the two-step route, Bloom 225 gave larger particles than Bloom 75 under matched conditions, consistent with the higher average molecular weight of the higher-Bloom material. Crosslinker dose produced a secondary effect in the same series: doubling the glutaraldehyde charge from 54 to 108µL reduced particle size for both Bloom grades, consistent with network densification and contraction during crosslinking. Acidic pH favored smaller particles, and acetone addition beyond the point of maximal recovery broadened the distribution. Confocal imaging showed FITC-gelatin-derived fluorescence associated with A549 cells within 24h. Gelatin Bloom number is therefore a practical, purchasable handle on relative particle size, and the preparations show preliminary evidence of association with a lung epithelial carcinoma line relevant to inhaled and systemic delivery.

Keywords: Gelatin nanoparticles, Desolvation, Bloom number, Glutaraldehyde, A549, Cellular association

Introduction

Nanoparticulate carriers built from natural polymers combine tunable size with degradability and low immunogenicity. Gelatin is among the most practical of these matrices: it is obtained by partial hydrolysis of collagen from skin, bone and tendon under acidic, alkaline or enzymatic conditions, is inexpensive and

widely available in pharmaceutical grade, and carries abundant side-chain functionality for crosslinking and conjugation [1-3]. Gelatin nanoparticles are conventionally prepared by desolvation, in which a water-miscible non-solvent is added to an aqueous gelatin solution until the polymer coils collapse and precipitate as dispersed spheres [4,5]. The single-step form of the process is simple but yields broad distributions when native gelatin is used, because low-molecular-weight fractions remain in solution and nucleate poorly. The two-step variant introduced by Coester and colleagues' addresses this by performing a first desolvation purely as a fractionation step: the low-molecular-weight material is discarded with the supernatant, and only the highmolecular-weight sediment is redissolved and desolvated again at acidic pH, giving smaller and more uniform particles [6]. Subsequent systematic work established temperature, pH, gelatin type, desolvating agent, and crosslinker concentration as the controlling variables [7], and the approach remains the reference method in current reviews of gelatin-based delivery systems, alongside more recent simplifications of the first step [8,9].

Two features of gelatin chemistry underlie this behavior. First, the material is polydisperse, and its molecular-weight distribution, reported commercially as Bloom number, a gel-strength index, governs both the stability of the resulting particles and their size [6,10,11]. Second, gelatin is amphoteric, so the distance of the working pH from the isoelectric point sets the chain charge and hence the degree of expansion at the moment of precipitation [7,12]. The particles must be stabilised or they redissolve when the desolvating agent is removed. Glutaraldehyde remains the most widely used crosslinker for this purpose because it reacts rapidly with lysine ε-amino groups through Schiff base formation and aldol condensation and is inexpensive. However, it can be cytotoxic through released aldehyde and requires thorough purification [13-15]. A549 human lung adenocarcinoma cells, derived from an alveolar type II-like epithelium [16], are a standard model for both inhaled delivery and lung-cancer nanomedicine, and gelatin carriers have since been developed specifically for pulmonary chemotherapy in this line [17,18]. The present work aimed to establish which synthesis parameters give reproducible relative control of gelatin nanoparticle size across two Bloom grades and both desolvation routes, and to obtain preliminary evidence of whether the resulting fluorescent preparations associate with A549 cells.

Materials and Methods

Materials

Type B bovine gelatin (Bloom 75 and Bloom 225), 25% aqueous glutaraldehyde, Fluorescein-5isothiocyanate (FITC), Hoechst 33342, and 1,1′-Dioctadecyl-3,3,3′,3′-Tetramethylindocarbocyanine Perchlorate (DiI) were obtained from Sigma-Aldrich (St. Louis, MO, USA). Acetone was obtained from VWR International (San Diego, CA, USA). Hydrochloric acid, sodium hydroxide, and deionized water were of analytical grade. RPMI-1640 medium and fetal bovine serum were used for cell culture; regenerated cellulose dialysis membrane was obtained from Fisher Scientific.

One-Step Desolvation

Gelatin (2g) was dissolved in deionized water to a total volume of 20mL with stirring at 60°C. The solution was adjusted to pH 2.5, and 25mL acetone was added dropwise with continued stirring at 60°C until the dispersion became opalescent. Glutaraldehyde (50μL of 25% aqueous solution) was then added and crosslinking allowed to proceed for 2h. The same crosslinker charge was used for both Bloom grades, so the one-step comparison between grades is internally controlled.

Two-Step Desolvation

Gelatin was dissolved as above. A first desolvation was performed by adding 25mL acetone; the dispersion was allowed to sediment over several minutes, and the supernatant containing low-molecular-weight fractions was discarded. The sediment was redissolved in 25mL water at 60°C, adjusted to pH 2.5, and a second desolvation was performed by dropwise addition of 40mL acetone. Glutaraldehyde (50, 54 or 108 μL of 25% aqueous solution) was added, and crosslinking was allowed to proceed for 2 hours for both the one- and two-step routes, then purified by dialysis (Section 2.5) and stored at 4–8°C. Both routes are summarised in Figure 1, below.

FITC-Labelled Gelatin Nanoparticles

A gelatin/FITC stock was prepared by dissolving 2.0g gelatin in 55mL borate–potassium chloride–sodium hydroxide buffer, adding 0.03g FITC, followed by 25mL acetone; the product was recovered by repeated centrifugation and stored for subsequent use. Aliquots of labeled gelatin were combined with unlabelled granular gelatin and incubated for several minutes before being taken through either desolvation route as described above.

Purification

Plain and fluorescent preparations (25–30mL) were transferred to a regenerated cellulose dialysis membrane and dialyzed against stirred deionized water over several days, with the external phase replaced periodically until the internal and external phases equilibrated, monitored by pH. Free-fluorophore content of the retentate after dialysis was not determined (Section 4) (Figure 1).

Particle Sizing and the Basis on Which Size is Reported

Hydrodynamic size was measured by dynamic light scattering (Nanotrac, Microtrac Inc.). Particle morphology and height were examined by atomic force microscopy in height mode, with line-scan profiles taken across individual particles. Absolute hydrodynamic diameters are not reported in this work. The archived light-scattering output for these preparations is not consistent with the physical characteristics of the samples, which were visibly opalescent during synthesis, were retained by a dialysis membrane, and were crosslinked, nor with the 100–300 nm range consistently reported for gelatin nanoparticles prepared by acetone desolvation

and aldehyde crosslinking [6-9,19]. Because the discrepancy cannot be resolved retrospectively, and because reporting values that are not physically plausible would misrepresent the preparations, size is reported here only as ordinal comparison between conditions measured on the same instrument under matched settings. Such comparisons are internally controlled and do not depend on absolute calibration. Re-measurement with zaverage and polydispersity index under ISO 22412 conditions, confirmed by an orthogonal numberweighted method, is identified as the priority for further work (Section 5).

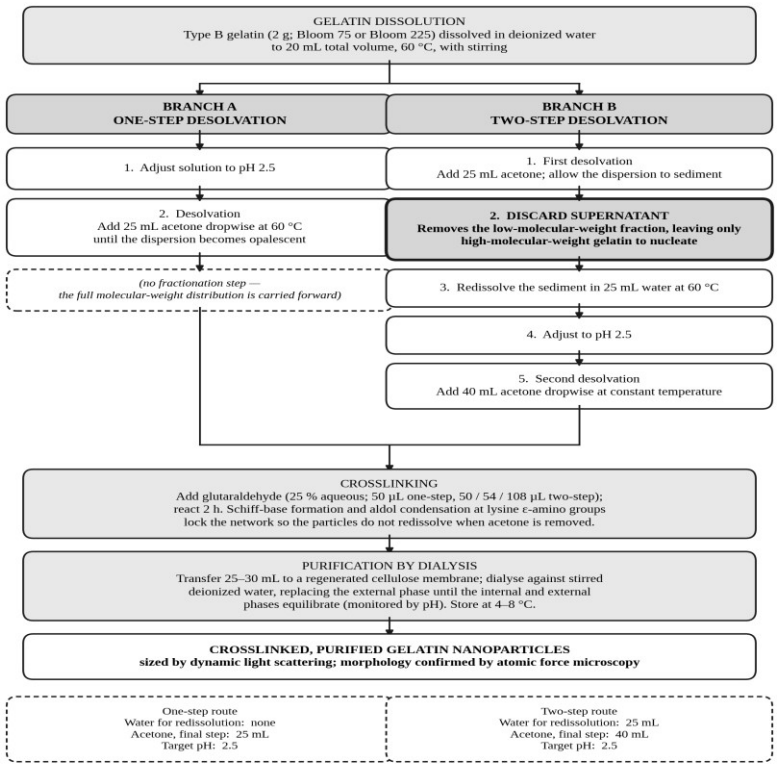

Figure 1: One-step and two-step branches side by side, showing where the first desolvation supernatant is discarded, where pH is adjusted, where glutaraldehyde enters, and the dialysis step. Reagent volumes are those used in this work.

Cell Culture and Uptake

A549 cells (2.5×10^4) were seeded onto 35 mm glass-bottom confocal dishes (MatTek Corporation, Ashland, MA, USA) in RPMI-1640 supplemented with 10% fetal bovine serum and cultured for 24h at 37°C in 5% CO_2. A low seeding density was used so that individual cells could be resolved. Medium was replaced with PBS for 1h, then with fresh medium, and cells were dosed with 50µL of concentrated FITCgelatin preparation in dialyzed water applied to the medium surface above the cell population. Dosed cultures were returned to the incubator and maintained for 24 h at 37°C in 5% CO_2. Nuclei were then counterstained with Hoechst 33342 and the plasma membrane with DiI. We followed thesupplierrecommended conditions inserted pending confirmation: Hoechst 33342 at 1–5µg/mL and DiI at 1–5µM, each for 10–20 min at 37°C, followed by washing with fresh medium, giving a three-channel preparation in which the FITC-labelled gelatin is imaged in the green channel. Fluorescence distribution was assessed by confocal laser scanning microscopy. Control dishes were handled identically but received no particles. A dose-matched free-FITC control was not performed (Section 4). The actual ranges and values for the confocal acquisition metadata were not recoverable at this time.

Results

Bloom Grade Determines the Direction of the Size Difference in Both Routes

Under matched conditions (60°C, pH 2.5, dropwise acetone addition, and identical glutaraldehyde charge), Bloom 225 gelatin gave larger particles than Bloom 75 in the one-step route, and the same ordering was reproduced in the two-step route. Bloom number is a gel-strength index that tracks the average molecular weight of the gelatin fraction, so the higher-Bloom material presents longer chains that collapse into larger desolvated aggregates. Because Bloom grade is specified at the point of purchase, this provides a coarse but reliable relative size control that requires no change to the process and no additional equipment.

Increasing Glutaraldehyde Dose Reduced Particle Size

In the two-step route, increasing the glutaraldehyde charge from 54 to 108µL reduced particle size for both Bloom 75 and Bloom 225. The direction of the effect is consistent with progressive densification: as intramolecular and intermolecular links form, the desolvated coil contracts and the hydrated network exclude more water. The same trend has been reported for gelatin nanoparticles crosslinked at increasing glutaraldehyde ratios [20]. Crosslinker dose therefore acts as a secondary adjustment within the range set by the choice of Bloom grade.

pH and Desolvating Agent Addition

Working at pH 2.5, well below the isoelectric point of Type B gelatin, gave smaller particles than less acidic conditions; the acidic condition was therefore maintained throughout. During dropwise acetone addition, the dispersion remained visually unchanged until the acetone-to-aqueous ratio approached unity, at which point a faint haze appeared, marking the onset of particle formation; the suspension became translucent and then milky as addition continued. Addition beyond the point at which recovery was maximal broadened the size distribution rather than increasing yield. Preparations could not be made below approximately 40°C, at which point the viscosity of the gelatin solution and the onset of coil–helix renaturation prevented controlled desolvation; 60°C was used throughout.

Particle Morphology by Atomic Force Microscopy

Atomic force microscopy of dried preparations showed discrete, well-separated, rounded features against a flat substrate, with no evidence of a continuous film or of fused aggregates (Figure 2). Height mode resolved individual particles across a range of sizes within a single 1µm × 1µm scan, and line-scan profiles taken across individual features gave single, symmetric peaks (Figure 3), consistent with isolated particles rather than surface debris. Because the samples were dried onto the substrate and because tip convolution broadens lateral dimensions, these images are reported here as morphological confirmation of discrete particle formation only; they are not used to assign absolute size, for the reason set out in Section 2.6 (Figure 2 & 3).

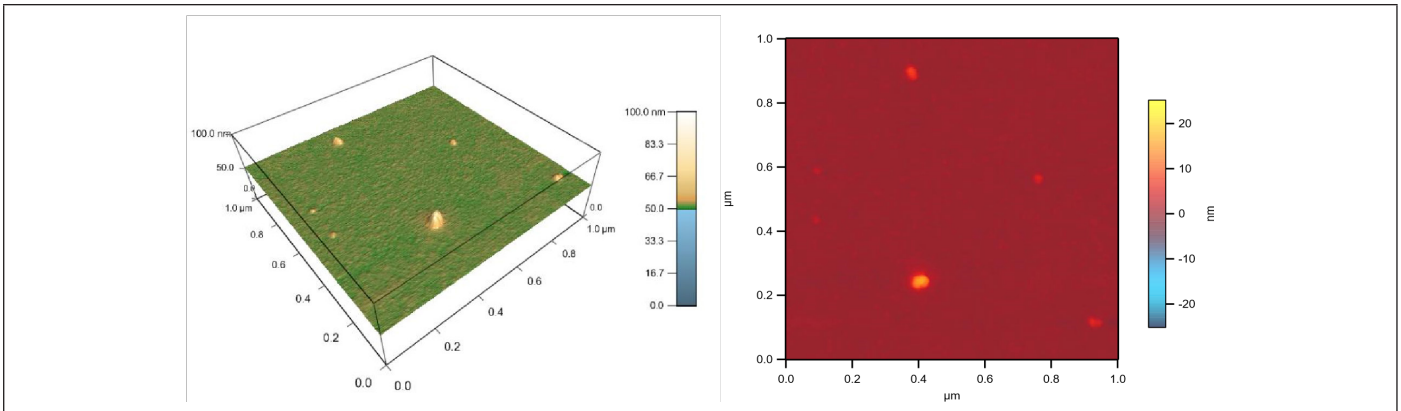

Figure 2: Atomic force microscopy of gelatin nanoparticles: three-dimensional height image (left) and the corresponding two-dimensional height image with z scale (right). Scan area 1 µm × 1 µm. Reproduced from the source thesis.

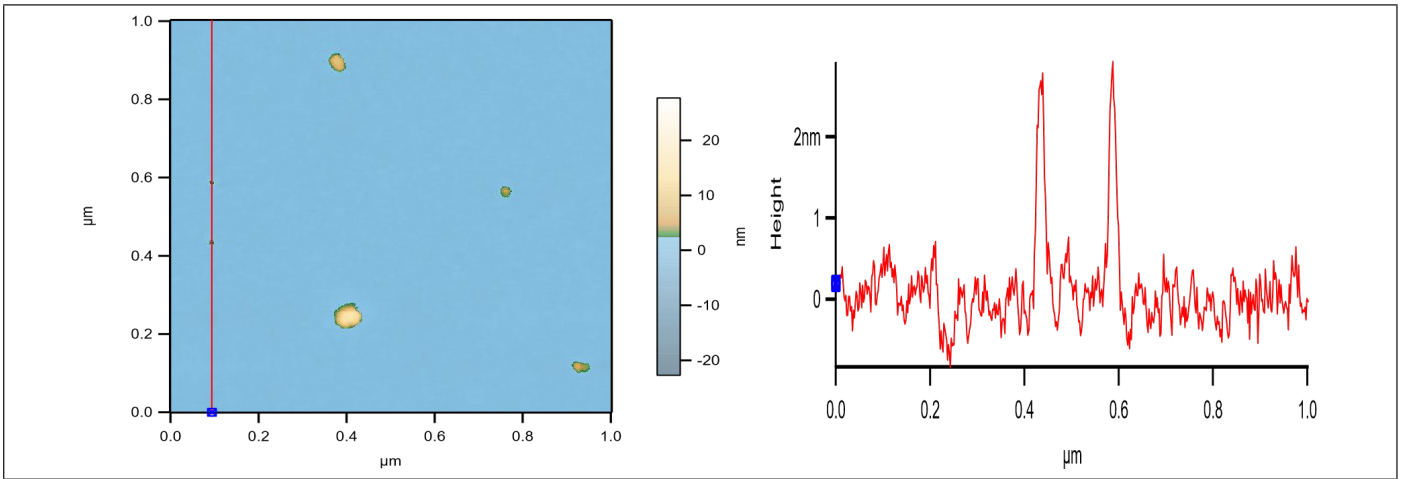

Figure 3: Representative atomic force microscopy height image with the line-scan path indicated (left) and the corresponding height profile across that line (right). Heights are subject to dehydration and tip-convolution bias and are not used to assign absolute particle size (Section 2.6). Reproduced from the source thesis.

Association Of FITC-Gelatin Preparations with A549 Cells

Control A549 cells showed the expected Hoechst and DiI counterstains with no green signal. After 24h exposure, cells dosed with the FITC-gelatin preparation showed extensive green fluorescence associated with the cell body (Figure 4). FITC-gelatin-derived fluorescence was therefore associated with A549 cells after 24h. Because no dose-matched free-fluorophore control was run and extracellular fluorescence was not quenched, particle-associated fluorescence was not separated from any released dye, and surface binding was not distinguished from internalization; the observation is accordingly reported as evidence of association rather than of uptake (Figure 4).

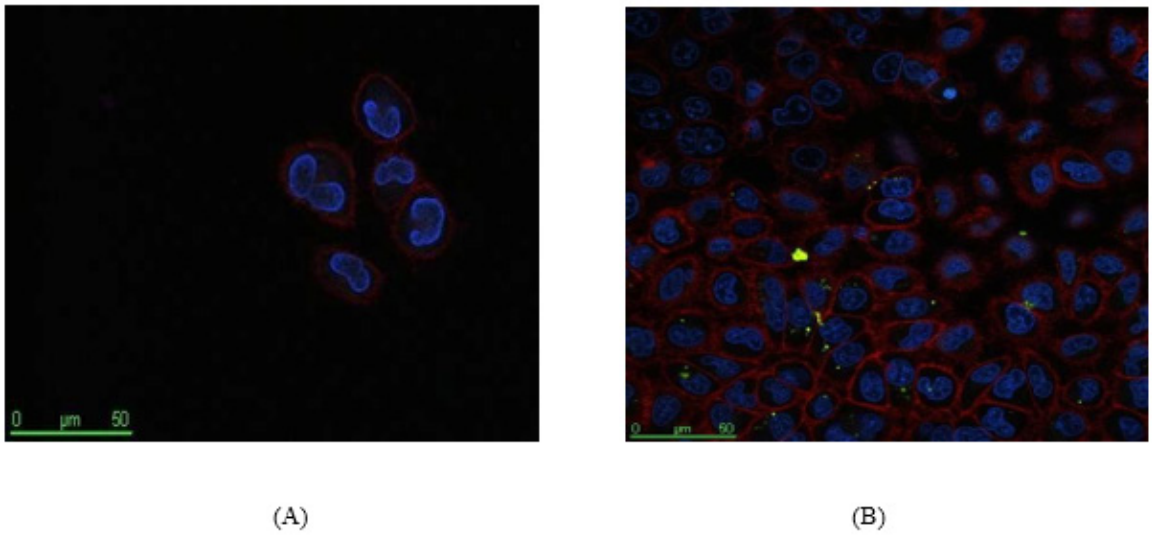

Figure 4: Confocal laser scanning microscopy of A549 cells. (A) Untreated control, showing Hoechst 33342stained nuclei (blue) and DiI-stained plasma membrane (red), with no green signal. (B) Cells 24 h after dosing with FITC-labelled gelatin preparation, showing green fluorescence associated with the cell body. Scale bar 50 µm. Surface binding is not distinguished from internalization on these data (Sections 3.5 and 4). Reproduced from the source thesis.

Discussion

The two dominant variables identified here, gelatin Bloom grade and crosslinker dose, act through different mechanisms and are therefore independently useful. Bloom number acts before particle formation, by setting the molecular-weight distribution of the material that precipitates; glutaraldehyde acts after, by contracting and locking the precipitated network. The consequence is a practical two-tier control scheme in which coarse size selection is made at the point of purchase and fine adjustment at the crosslinking step, avoiding reliance on solvent addition rate, the parameter most sensitive to operator technique. This interpretation is consistent with the finding that gelatin molecular weight determines the stability of twostep desolvated particles [6] and with subsequent parametric studies of the same process [7,8]. The value of these comparisons does not depend on absolute size calibration. Each contrast reported here, Bloom 225 against Bloom 75, 108µL glutaraldehyde against 54µL, pH 2.5 against less acidic conditions, was measured on the same instrument under matched settings, so systematic error affects both arms equally, and the ordering is preserved. What such data cannot support is placement of these preparations within the size ranges associated with particular uptake pathways, and no such placement is attempted here. The limits of that approach should be stated plainly. A single light-scattering modality determined size; a single lightscattering modality determined size; z-average and polydispersity index were not recorded, and absolute diameters are not reported for the reason given in Section 2.6, so these preparations cannot be assigned to a defined size range. Atomic force microscopy (Figures 2 and 3) confirms that discrete particles formed, but it was performed on dried samples and is subject to tip convolution, so it does not supply an independent absolute size. Zeta potential was not determined, leaving the colloidal description of an amphoteric matrix incomplete.

Establishing absolute size would address that line of interpretation, which is where the biological value of this system lies. A549 cells express both clathrin heavy chain and caveolin-1 and internalize nanoparticles by clathrin-mediated, caveolae-mediated, and macropinocytic routes in parallel, with the balance depending on particle size and surface chemistry [21,22]. Particles in the 100–200 nm range are the most efficiently endocytosed by this line in passive-targeting studies [17], and genipin-crosslinked gelatin nanocarriers loaded with a hydrophobic payload have been shown to enter A549 cells specifically through caveolaemediated endocytosis [19]. Once size is established on a calibrated basis,

the present preparations can be positioned against that literature and the entry route tested directly. The present cell observation carries corresponding constraints. Association is demonstrated qualitatively at a single time point; no dosematched free-fluorophore control, extracellular quenching step, orthogonal z-stack reconstruction, or lowtemperature incubation was performed, so internalization was not established, and the entry route was not identified. No viability assay accompanied the imaging, so avid association cannot be distinguished from uptake by compromised cells. A further caveat attaches to the membrane counterstain itself: DiI is a lipophilic carbocyanine that is progressively internalized through normal membrane turnover, so over a 24 h incubation the red channel no longer reports the plasma membrane exclusively, and apparent colocalization of green and red signal cannot by itself be read as intracellular delivery.

Crosslinker choice is the clearest opportunity to develop this system further. Glutaraldehyde is efficient and inexpensive but is the principal toxicological liability of the formulation, and the field has moved substantially toward alternatives: genipin, which is markedly less cytotoxic and is now well characterized in nanomedicine oncology applications [19,23]; carbodiimide chemistry, which forms zero-length amide links without incorporating the crosslinker into the product; and enzymatic crosslinking. Because companion work in this laboratory has established genipin handling for gelatin scaffolds, preparing a genipin-crosslinked arm of the same nanoparticle series is a direct and low-cost extension. Two reporting gaps bear on that development. Residual glutaraldehyde after dialysis was not quantified, which is a material omission for any preparation intended for cell work, and batch yield, inter-batch reproducibility, payload encapsulation, and release behavior were not determined. The study is accordingly presented as a preliminary parametric comparison rather than as a characterized delivery system.

Conclusions

Gelatin nanoparticles were prepared from Type B gelatin of two Bloom grades by both one-step and twostep desolvation and stabilized with glutaraldehyde. Bloom grade determined the direction of the size difference in both routes, with Bloom 225 giving larger particles than Bloom 75 under matched conditions, and increasing glutaraldehyde dose produced a further size reduction consistent with network contraction. Acidic pH favored smaller particles, and excess desolvating agent broadened the distribution. Size effects are reported as internally controlled ordinal comparisons; absolute diameters are not reported. FITC-gelatinderived fluorescence was associated with A549 lung adenocarcinoma cells within 24h, providing preliminary support for further evaluation of gelatin carriers in this cell type. Calibrated re-measurement of particle size is the immediate requirement: z-average with polydispersity index under ISO 22412 conditions, intensity- and number-weighted distributions with dispersant, refractive index, temperature and run count stated, confirmed by an orthogonal number-weighted method such as nanoparticle tracking analysis or transmission electron microscopy, together with zeta potential as a function of pH and ionic strength [6-9,12,19,21,23-25]. On the cell side, a dose-matched free-fluorophore control, extracellular quenching with orthogonal z-stack reconstruction, a 4°C incubation and a viability assay would convert the present observation into a supported uptake result, with flow cytometry and a pharmacological inhibitor panel then rendering uptake quantitative and assigning the entry route [21,22]. For the formulation itself, substituting genipin or carbodiimide chemistry for glutaraldehyde, quantifying and quenching residual aldehyde, reporting batch yield and inter-batch variation, and loading a model therapeutic with characterization of release would convert the carrier into a delivery system suitable for evaluation in pulmonary or locoregional models [13,15,17,18,19,26].

Author Contributions, Funding, Competing Interests and Data Availability

Emmanuella Rony was responsible for conducting all experiments, data collection, analysis and recording, and primary written work. Adrian McCollum assisted with analysis, reviewing of written work, and some data collection. Jesse Edwards was primarily responsible for funding and project design and assisted with writing and analysis. Jillian Pope is the corresponding author responsible for reviewing, editing, and analyzing the final product. There are no competing interests with this work. Light stacking and image work can be found and documented in the document: Rony, E. Gelatin as tissue engineering scaffolding and potential drug delivery applications (M.S. thesis, Florida A&M University, defended 11 April 2011; 93 pp., ~15,200 words). Florida A&M University Library. This work was funded in part by FAMU Title III and the University of Florida, SEAGEP, Grant # HRD-0450279.

Acknowledgements

Dr. Scott C. Brown from the Particle Engineering Research Center (PERC) at the University of Florida for the training he provided. Mike Feen, a student in the chemistry department at UF; the Alliance for Graduate Education and the Professoriate (SEAGEP) at the University of Florida (UF) staff: Dr. Anne E. Donnelly, Dr Samesha Barnes, and Dr Tara Washington. Dr. Nelly Mateeva for her support. Many thanks go to the University of Florida and Florida A&M University for the use of their facilities. Last but not least, I would also like to thank Basant Nassar for being such a great friend and editor.

References

1. Schwick HG, Heide K (1969) Immunochemistry and immunology of collagen and gelatin. Bibl Haematol 33: 111–125.
2. Young S, Wong M, Tabata Y, Mikos AG (2005) Gelatin as a delivery vehicle for the controlled release of bioactive molecules. J Control Release 109(1–3): 256–274.
3. Salata OV (2004) Applications of nanoparticles in biology and medicine. J Nanobiotechnology 2(1): 3.

4. Marty JJ, Oppenheim RC, Speiser P (1978) Nanoparticles-a new colloidal drug delivery system. Pharm Acta Helv 53(1): 17–23.
5. Quintanar Guerrero D, Allémann E, Fessi H, Doelker E (1998) Preparation techniques and mechanisms of formation of biodegradable nanoparticles from preformed polymers. Drug Dev Ind Pharm 24(12): 1113–1128.
6. Coester CJ, Langer K, Von Briesen H, Kreuter J (2000) Gelatin nanoparticles by two step desolvation-a new preparation method, surface modifications and cell uptake. J Microencapsul 17(2): 187–193.
7. Azarmi S, Huang Y, Chen H, McQuarrie S, Abrams D, et al. (2006) Optimization of a two-step desolvation method for preparing gelatin nanoparticles and cell uptake studies in 143B osteosarcoma cancer cells. J Pharm Pharm Sci 9(1): 124–132.
8. Francesca Milano, Annalia Masi, Marta Madaghiele, Alessandro Sannino, Luca Salvatore, et al. (2023) Current trends in gelatin-based drug delivery systems. Pharmaceutics 15(5): 1499.
9. Khramtsov P, Burdina O, Lazarev S, Novokshonova A, Bochkova M, et al. (2021) Modified desolvation method enables simple one-step synthesis of gelatin nanoparticles from different gelatin types with any bloom values. Pharmaceutics 13(10): 1537.
10. Farrugia CA, Groves MJ (1999) Gelatin behavior in dilute aqueous solution: designing a nanoparticulate formulation. J Pharm Pharmacol 51(6): 643–649.
11. Meyer M, Morgenstern B (2003) Characterization of gelatine and acid soluble collagen by size exclusion chromatography coupled with multi angle light scattering (SEC-MALS). Biomacromolecules 4(6): 1727–1732.
12. Bhattacharjee S (2016) DLS and zeta potential-what they are and what they are not. J Control Release 235: 337–351.
13. Migneault I, Dartiguenave C, Bertrand MJ, Waldron KC (2004) Glutaraldehyde: behavior in aqueous solution, reaction with proteins, and application to enzyme crosslinking. Biotechniques 37(5): 790–802.
14. Zwiorek K, Kloeckner J, Wagner E, Coester C (2004) Gelatin nanoparticles as a new and simple gene delivery system. J Pharm Pharm Sci 7(4): 22–28.
15. Friess W (1998) Collagen-biomaterial for drug delivery. Eur J Pharm Biopharm 45(2): 113–136.
16. Giard DJ, Aaronson SA, Todaro GJ, Arnstein P, Kersey JH, et al. (1973) *In vitro* cultivation of human tumors: establishment of cell lines derived from a series of solid tumors. J Natl Cancer Inst 51(5): 1417– 1423.
17. Hend Abdelrady, Rania M Hathout, Rihab Osman, Imran Saleem, Nahed D Mortada (2019) Exploiting gelatin nanocarriers in the pulmonary delivery of methotrexate for lung cancer therapy. Eur J Pharm Sci 133: 115-126.
18. Xianchao Jiang, Zhen Du, Xinran Zhang, Fakhar Zaman, Zihao Song (2023) Gelatin-based anticancer drug delivery nanosystems: a mini review. Front Bioeng Biotechnol 11: 1158749.
19. Das RP, Nayak M, Singh BG, Majee K, Kunwar A (2026) Effect of genipin crosslinking on the cellular delivery of gelatin nanocarriers using curcumin as a payload. Int J Biomater 9512576.
20. Cascone MG, Lazzeri L, Carmignani C, Zhu Z (2002) Gelatin nanoparticles produced by a simple method without emulsion as a delivery system for methotrexate. J Mater Sci Mater Med 13(5): 523–526.
21. ISO 22412:2017. Particle size analysis-dynamic light scattering (DLS). Geneva: International Organization for Standardization.
22. Kuhn DA, Vanhecke D, Michen B, Blank F, Gehr P, et al. (2014) Different endocytotic uptake mechanisms for nanoparticles in epithelial cells and macrophages. Beilstein J Nanotechnol 5: 1625–1636.
23. Faria M, Björnmalm M, Thurecht KJ, Stephen J Kent, Robert G Parton, et al. (2018) Minimum information reporting in bio–nano experimental literature. Nat Nanotechnol 13(9): 777–785.
24. Arnold Sipos, Kwang Jin Kim, Constantinos Sioutas, Edward D Crandall (2019) Evidence for nanoparticle-induced lysosomal dysfunction in lung adenocarcinoma (A549) cells. Int J Mol Sci 20(21): 5253.
25. Natalia Farkas, John A Kramar (2021) Dynamic light scattering distributions by any means. J Nanopart Res 5: 10.
26. Tanuj Sharma, Simranjit Kaur, Jai Bharti Sharma, Shadma Wahab, Devesh U Kapoor (2026) Harnessing genipin as a biocompatible crosslinker in nanomedicine for oncology applications. 3 Biotech 16(5): 186.